Supplementary Technical Report
A Geometric Perspective on Structured Light Coding

Mohit Gupta and Nikhil Nakhate

Department of Computer Sciences, University of Wisconsin-Madison, USA
mohitg@cs.wisc.edu, nakhate@wisc.edu

In this technical report, we provide supporting derivations and additional results for the ECCV 2018 paper titled "A Geometric Perspective on Structured Light Coding".

1 Derivation for the Surrogate Metric Υ

The expected correspondence error (ECE) metric of a structured light (SL) coding scheme, as derived in Eq. 3 of the main paper, is difficult to use as an objective function for SL code optimization. This is because the resulting optimization problem has no known analytical solution. It is expensive to even compute the ECE numerically, due to the double integral, each taken over a high-dimensional space (unknown space and measured intensity space). In order to perform the optimization, we derive a surrogate objective function based on a first order differential analysis of the image formation equation (Eq. 1 in the main paper). This surrogate is similar in spirit to the surrogate metric derived for designing time-of-flight coding schemes [1], where an optimization analysis was performed in the temporal domain of the coding functions. In this work, we perform the analysis in the spatial domain for design of spatially coded SL patterns.

We start by taking the partial derivative of the intensity I_i (in Eq. 1 of the main paper) with respect to the projector correspondence c:

$$\frac{\partial I_i}{\partial c} = \alpha \, P_i'(c) \, ,$$

where $P_i'(c)$ is the derivative of the pattern coding function $P_i(c)$. We assume that the albedo factor α is independent of the projector correspondence c. In practice, α depends on scene depths (and thus, projector correspondence). Such dependence can be absorbed into the function $P_i(c)$. The partial derivative of the intensity measurement vector $\mathbf{I} = [I_1, I_2, \ldots, I_K]$, with respect to c, is given as:

$$\left| \frac{\partial \mathbf{I}}{\partial c} \right| = \sqrt{\sum_{i=1}^{K} \left(\frac{\partial I_i}{\partial c} \right)^2} = \alpha \sqrt{\sum_{i=1}^{K} P_i'(c)^2} \, .$$

By rearranging terms, we get:

$$|\partial c| = \frac{|\partial \mathbf{I}|}{\alpha \sqrt{\sum_{i=1}^{K} P_i'(c)^2}} \, . \tag{1}$$

This equation expresses the differential correspondence error $|\partial c| = |\widehat{c} - c|$ due to small measurement noise $|\partial \mathbf{I}| = \sqrt{\sum_{i=1}^{K} \partial I_i^2}$, where I_i is the true measured intensity, and I_i' is the actual measured intensity due to noise, and $\partial I_i = I_i' - I_i$. Let the standard deviations of the random variables $|\partial \mathbf{I}|$ and $|\partial c|$ be ς and σ_c, respectively. Then, from Eq. 1, it follows that ς and σ_c are related as:

$$\sigma_c = \frac{\varsigma}{\alpha \sqrt{\sum_{i=1}^{K} P_i'(c)^2}} \,. \tag{2}$$

Let $\Psi = \frac{1}{\sigma_c}$ be the reciprocal of the correspondence standard deviation σ_c, for a given unknown point P_U. Since Ψ is the inverse of correspondence standard deviation, larger the value of Ψ, lower is the correspondence error. $\Psi(P_U)$ is given as:

$$\Psi(P_U) = \frac{1}{\sigma_c} = \frac{\alpha \sqrt{\sum_{i=1}^{K} \mathcal{P}_i'(c)^2}}{\varsigma} \,. \tag{3}$$

The mean Ψ of a coding scheme $\mathcal{C}$ is given by averaging $\chi(P_U)$ over the space of all unknowns:

$$\Psi = \frac{1}{\mathbf{V_U}} \int\limits_{c,\alpha,A} \Psi(P_U) \; dA \, d\alpha \, dc \,, \tag{4}$$

where $\mathbf{V_U}$ is the volume of the unknown space. Substituting Eq. 3 into Eq. 4, and simplifying with the assumption that the noise standard deviation is a constant, we get:

$$\Psi = \frac{\alpha_{mean} \int_c \sqrt{\sum_{i=1}^{K} P_i'(c)^2} \; dc}{\varsigma \; N_C} \,, \tag{5}$$

where N_c is the number of projector columns, and α_{mean} is the mean albedo factor over the space of unknowns. The term $\int \sqrt{\sum_{i=1}^{K} P_i'(c)^2} \; dc$ is equal to the length of the coding curve Λ of the coding scheme (as defined in the main paper). Substituting in Eq. 5, we get:

$$\Psi = \frac{\alpha_{mean} \Lambda}{\varsigma \; N_C} \,. \tag{6}$$

Since Ψ is defined as the inverse of the differential correspondence error (Eq. 3), we define the surrogate metric Υ as inverse of Ψ:

$$\Upsilon = \frac{1}{\Psi} \propto \frac{\varsigma}{\alpha_{mean} \Lambda} \,, \tag{7}$$

which is Eq. 4 in the main paper.

2 Additional Results and 3D Time Lapse Scanning

In the following pages, we show additional results, including comparisons for a 3D time lapse sequence captured under varying ambient light.

References

1. Gupta, M., Velten, A., Nayar, S., Breitbach, E.: What Are Optimal Coding Functions for Time-of-Flight Imaging? ACM Transactions on Graphics **37**(2) (2018)

Additional Results and Comparisons

Comparisons: K = 4

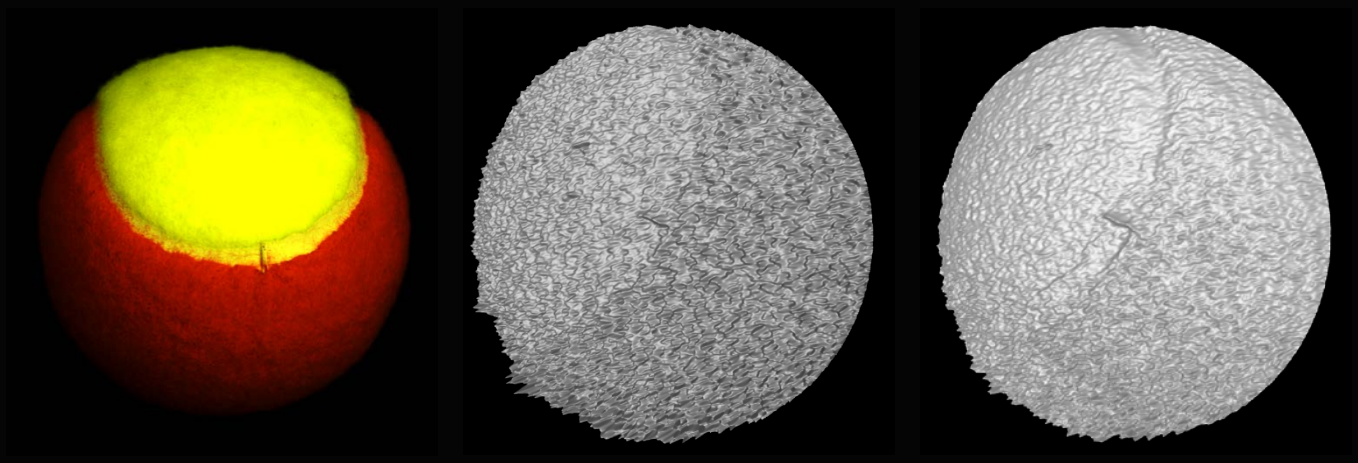

Scene | Sinusoid Coding | Hamiltonian Coding

Hamiltonian coding recovers details such as the seam on the ball

Comparisons: K = 4

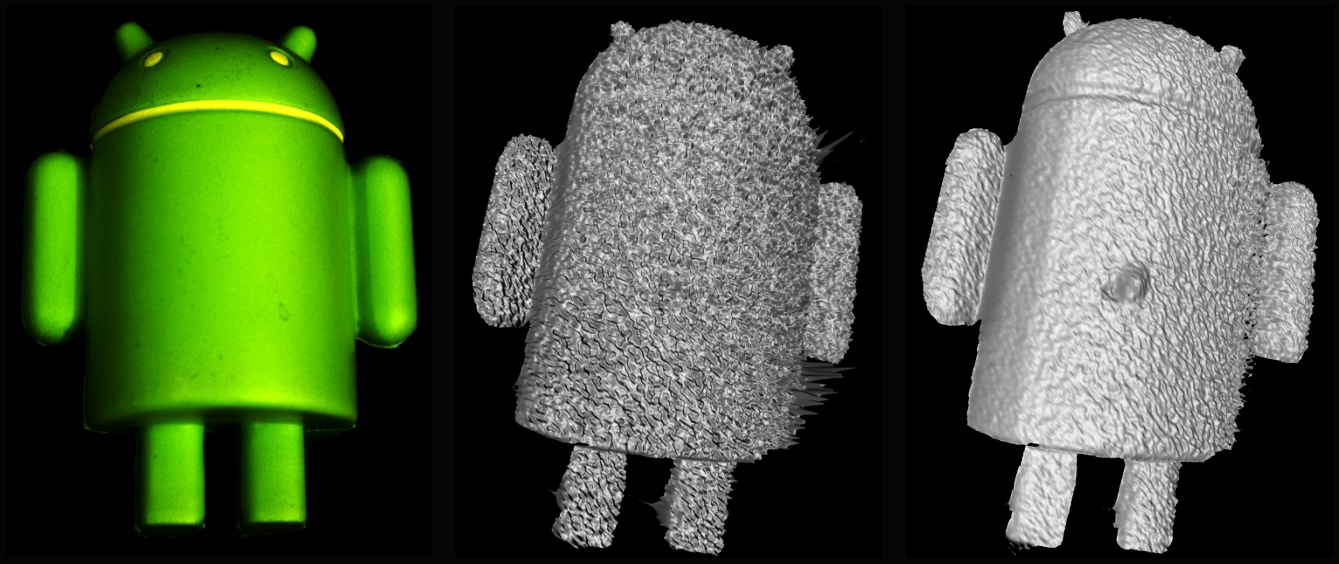

Scene | Sinusoid Coding | Hamiltonian Coding

Hamiltonian coding recovers details such as the seam on the android

Time-Lapse 3D Scanning

Imaging Setup

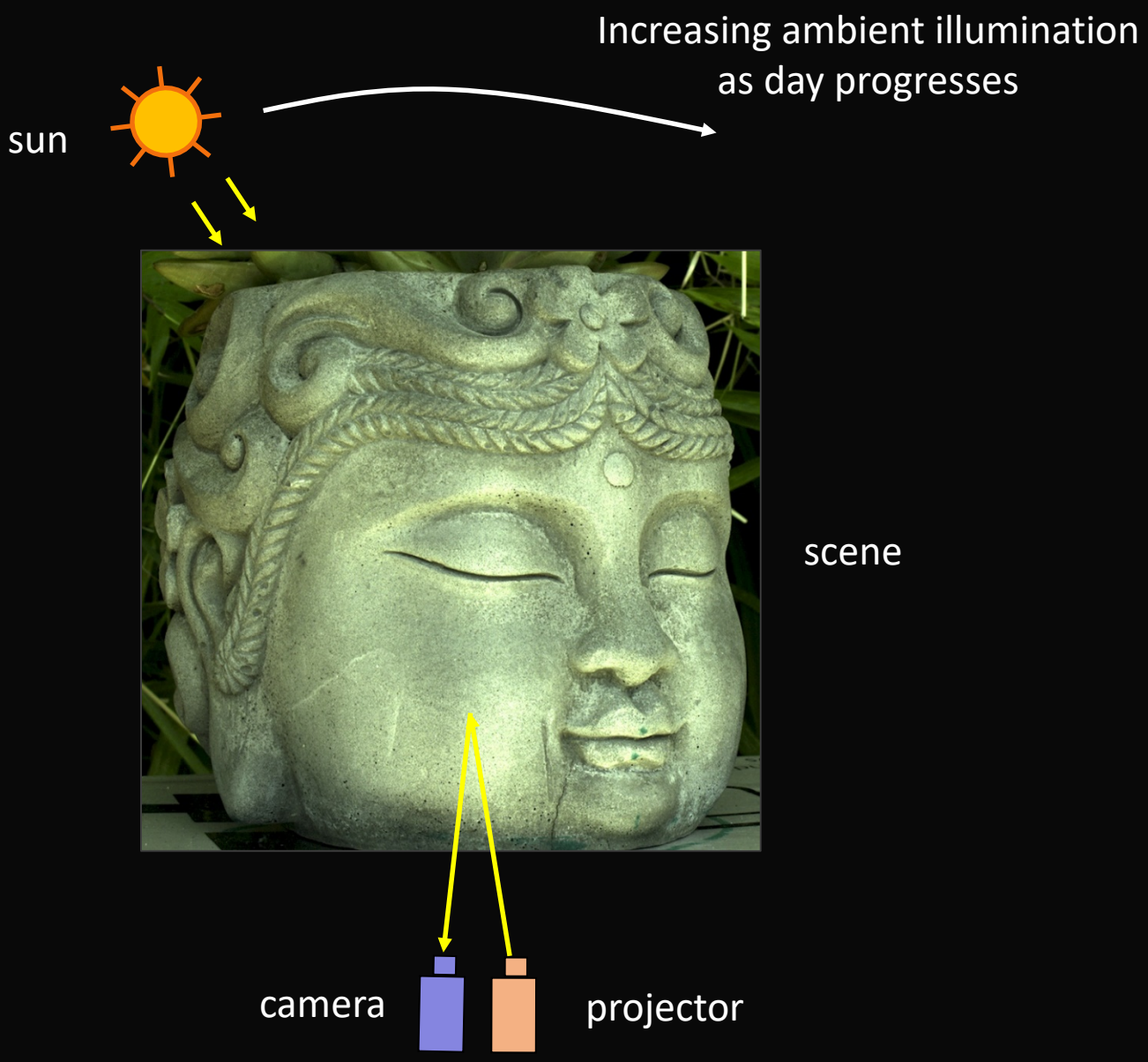

We Captured 3D Scans at
1 Hour Intervals from 6 AM to 1 PM

As the Day Progressed…
Ambient Illumination Increased and the SNR Decreased
(Projector Strength and Capture Time were Held Constant)

Input Images

6 AM

8 AM

10 AM

12 PM

Increasing Ambient Illumination

Decreasing Pattern Contrast and SNR

Following pages show comparisons for two schemes:

1. Multi-Frequency Sinusoid Coding for K=5
   - Three sinusoids at unit frequency, two at high frequency (see paper for details)

2. Hamiltonian Coding for K=5

3D Scanning Results: Multi-Frequency Sinusoid Coding

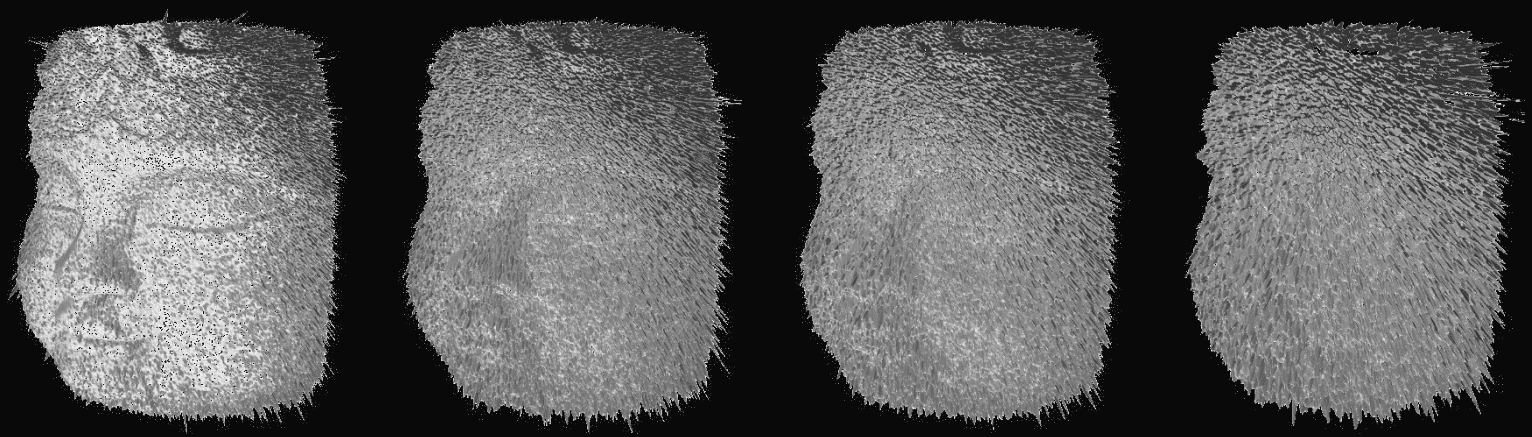

6 AM 8 AM 10 AM 12 PM

Reconstruction Quality Deteriorates Rapidly Due to Unwrapping Errors

3D Scanning Results: Hamiltonian Coding

6 AM 8 AM 10 AM 12 PM

Reconstruction Quality Degrades Gracefully

Side-by-Side Comparison [6 AM]

Multi-Frequency Sinusoid

Hamiltonian

Side-by-Side Comparison [7 AM]

Multi-Frequency Sinusoid

Hamiltonian

Side-by-Side Comparison [8 AM]

Large Unwrapping Errors due to Low SNR

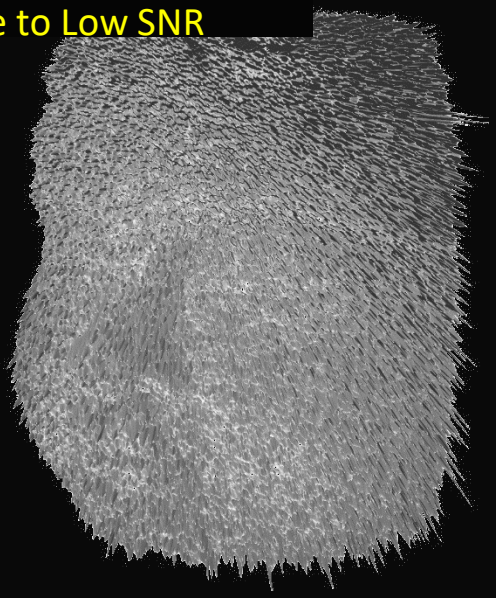

Multi-Frequency Sinusoid

Reconstruction Quality Degrades Gracefully

Hamiltonian

Side-by-Side Comparison [9 AM]

Large Unwrapping Errors due to Low SNR

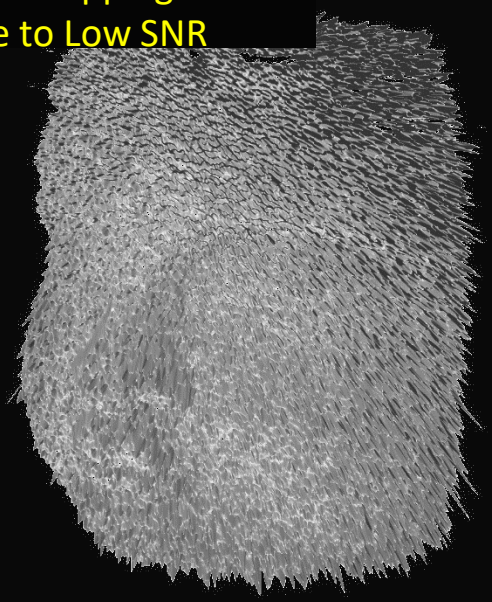

Multi-Frequency Sinusoid

Reconstruction Quality Degrades Gracefully

Hamiltonian

Side-by-Side Comparison [10 AM]

Large Unwrapping Errors due to Low SNR

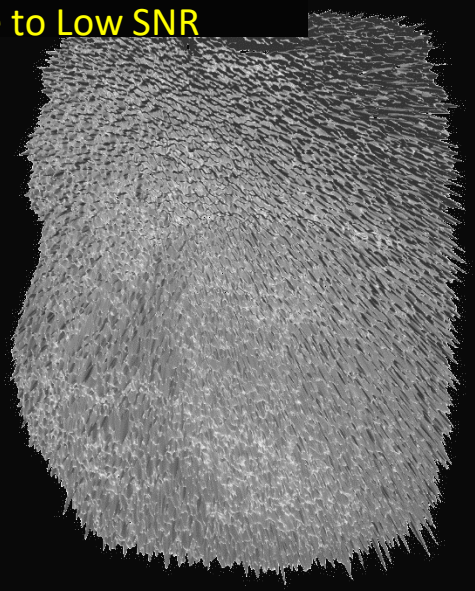

Multi-Frequency Sinusoid

Reconstruction Quality Degrades Gracefully

Hamiltonian

Side-by-Side Comparison [11 AM]

Large Unwrapping Errors due to Low SNR

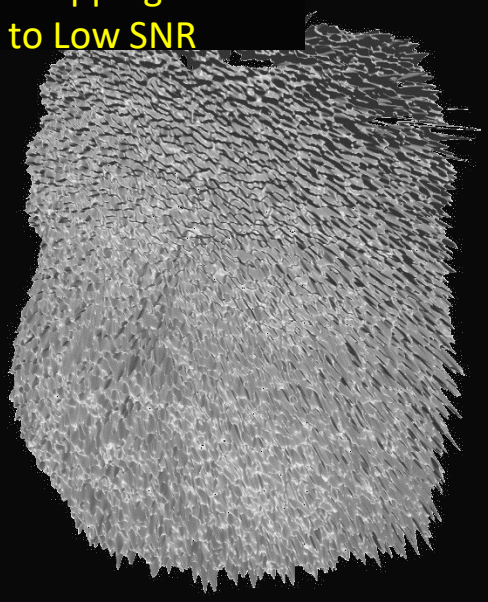

Multi-Frequency Sinusoid

Reconstruction Quality Degrades Gracefully

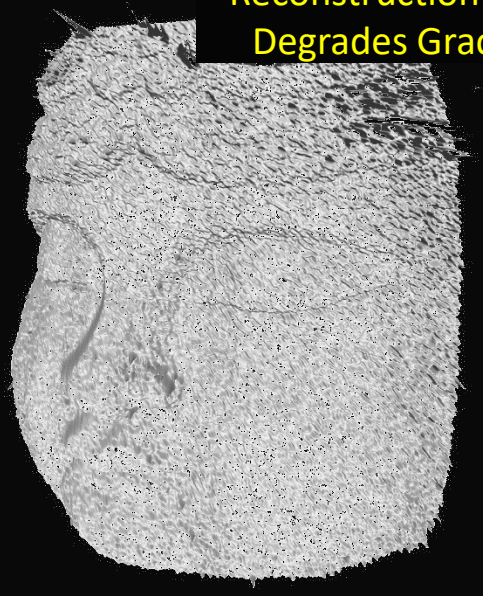

Hamiltonian

Side-by-Side Comparison [12 PM]

Large Unwrapping Errors due to Low SNR

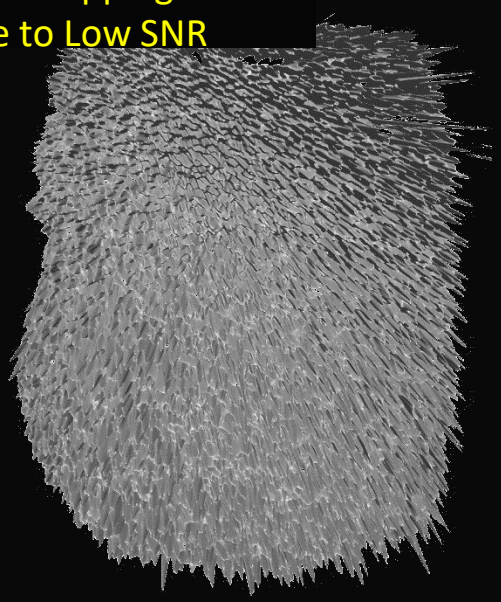

Multi-Frequency Sinusoid

Reconstruction Quality Degrades Gracefully

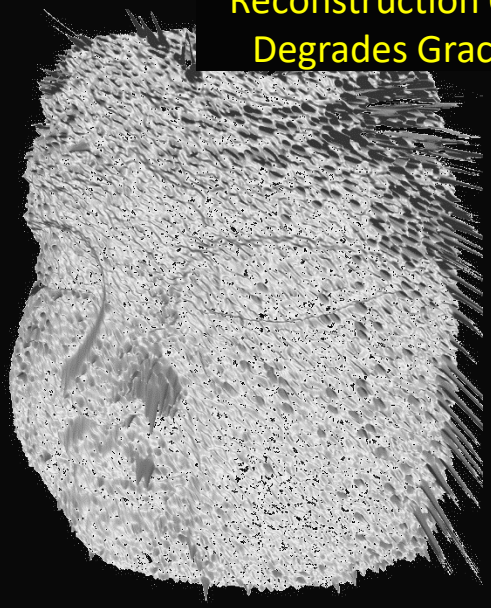

Hamiltonian

Side-by-Side Comparison [1 PM]

Large Unwrapping Errors due to Low SNR

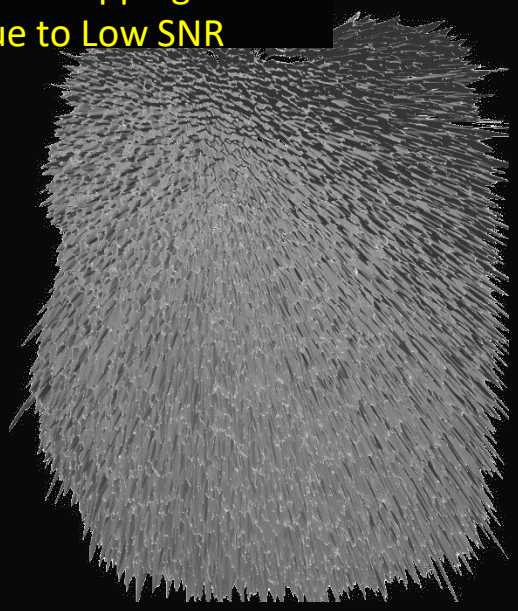

Multi-Frequency Sinusoid

Reconstruction Quality Degrades Gracefully

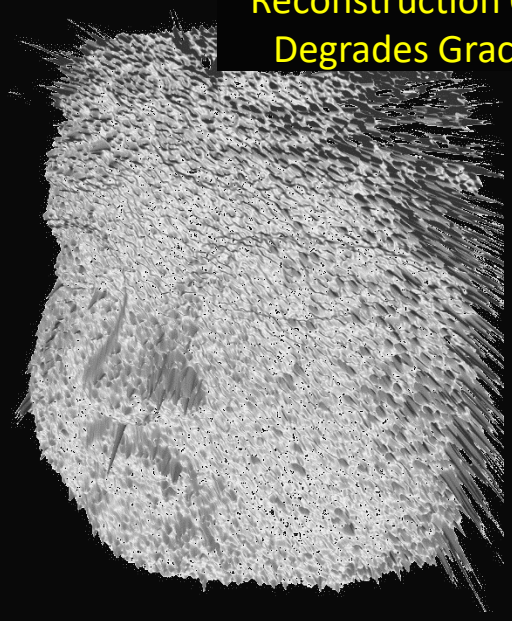

Hamiltonian